THE ASTROPHYSICAL JOURNAL, 413:604–610, 1993 August 20


# 30 DORADUS: ULTRAVIOLET AND OPTICAL STELLAR PHOTOMETRY

JESSE K. HILL,[1] RALPH C. BOHLIN,[2] KWANG-PING CHENG,[3,4] MICHAEL N. FANELLI,[3] PAUL HINTZEN,[5,4,6]
ROBERT W. O'CONNELL,[7] MORTON S. ROBERTS,[8] ANDREW M. SMITH,[5]
ERIC P. SMITH,[5,4] AND THEODORE P. STECHER[5]
*Received 1992 November 11; accepted 1993 February 26*

## ABSTRACT

Stellar photometry is presented for 314 stars in a 9.′7 × 9.′7 field in the 30 Dor nebula centered on R136. Magnitudes are computed from Ultraviolet Imaging Telescope images in up to 4 bands with effective wavelengths from 1615 to 2558 Å, and from a ground-based CCD image in the *B* band. Spectral types and extinctions are estimated using a least-squares technique, based on a spectrophotometric library compiled from *IUE* spectra. The fit spectral types agree to one library spectral type bin and two luminosity classes with types determined from optical slit spectra, for 34 of 39 non-WR stars. Approximately 35% of the 314 stars are fitted to main-sequence spectral types earlier than B1. Extinction of the more reddened stars in 30 Dor is shown to follow the Fitzpatrick 30 Dor extinction curve combined with a nebular curve of Fitzpatrick and Savage, where $E(B-V)$ for each component is determined by the least-squares fit. Assuming a foreground extinction of $E(B-V) = 0.10$, average values of the color excess internal to 30 Dor are $E(B-V)_F = 0.11 \pm 0.02$, from the Fitzpatrick 30 Dor extinction curve component, and $E(B-V)_{FS} = 0.17 \pm 0.17$ from the Fitzpatrick and Savage nebular extinction curve component. Most stars within the high surface brightness area centered near R136 have low nebular extinction [$E(B-V)_{FS} < 0.03$], while stars outside this area typically have $E(B-V)_{FS} < 0.30$. Dust grains following the nebular extinction curve may have been expelled from the central regions of 30 Dor by stellar winds, or stars in the outer regions may be behind or within dust clouds. We also suggest that the difference between the Galactic extinction curve and the Fitzpatrick 30 Dor extinction curve may result from the lower cumulative nucleosynthesis in the LMC and the long time necessary for the component producing the local maximum at 2200 Å (presumably carbon) to reach the interstellar medium in the form of grains.

*Subject headings:* dust, extinction — ISM: individual (30 Doradus) — Magellanic Clouds — techniques: photometric — ultraviolet: stars

## 1. INTRODUCTION

The 30 Dor region of the LMC contains the largest collection of very early type stars in the local group and is of considerable interest for studies of the formation and evolution of massive stars. Melnick (1985) determined spectral types for 69 stars in 30 Dor, using optical slit spectra. Spectral types for other stars in the region have been determined by Walborn (1986), Walborn & Blades (1987), and Parker (1992). Parker (1992) recently determined *UBV* magnitudes for 3400 stars in the 30 Dor region.

Extinction curves have been determined by Fitzpatrick & Savage (1984) and Fitzpatrick (1985), from *IUE* spectra of stars in the region. The Fitzpatrick (1985) 30 Dor curve is thought to apply over a region about a degree in extent, while the curve of Fitzpatrick & Savage (1984) is thought to apply primarily to a region a few arcminutes across at the core of the nebula. These curves differ significantly from each other, and from the mean extinction law derived for our Galaxy (Savage & Mathis 1979).

During the 1990 *Astro 1* Spacelab mission, the Ultraviolet Imaging Telescope (UIT) obtained 16 exposures centered on the 30 Dor nebula. Images were obtained (mostly on the daylight side of the orbit) in four intermediate-width bands, denoted B5, A2, A4, and A5, ranging in effective wavelength from 1615 to 2558 Å. Preliminary results obtained in a study utilizing the UIT 30 Dor images, plus images of a nearby field centered on SN 1987A and a field centered on the SNR 49A + B were presented by Cheng et al. (1992). This study presents results derived from stellar photometry of more than 300 stars in the four UV bands and the *B* band in a 9.′7 × 9.′7 field centered on R136, thereby allowing an investigation of the angular distribution of the amount of extinction following each of the two curves.

## 2. UIT AND GROUND-BASED IMAGES

Table 1 gives the image numbers of the UIT images used in this investigation, together with the filter and the exposure time in seconds. The procedure by which the UIT film images are reduced to flux-calibrated arrays of integers is described in Stecher et al. (1992). Large-format CCD images of 30 Dor were also obtained at the Cerro Tololo Inter-American Observatory (CTIO) 0.9 m telescope in the *U*, *B*, *R*, *u*, and Hα bands. Stellar photometry performed using the *B*-band image is utilized together with the UIT magnitudes in the spectral type and reddening fits. Astrometric solutions are derived for all images

[1] Hughes STX, 4400 Forbes Blvd, Lanham, MD 20706.
[2] Space Telescope Science Institute, Homewood Campus, Baltimore, MD 21218.
[3] NRC Postdoctoral Fellow, NASA/GSFC, Greenbelt, MD 20771.
[4] Visiting Astronomer at the Kitt Peak National Observatory of the NOAO operated by AURA, Inc., under contract to the NSF.
[5] Laboratory for Astronomy and Solar Physics, NASA/GSFC, Greenbelt, MD 20771.
[6] Department of Physics and Astronomy, California State University, Long Beach, CA 90840.
[7] University of Virginia, P.O. Box 3818, Charlottesville, VA 22903.
[8] National Radio Astronomy Observatory, Operated by Associated Universities Inc. under cooperative agreement with the NSF, Edgemont Rd., Charlottesville, VA 22903.

TABLE 1

UIT IMAGES USED FOR 30 DOR STELLAR PHOTOMETRY

| UIT Image | Exposure Time (s) | UIT Bandpass | λ (Å) | Bandwidth (Å) |
|---|---|---|---|---|
| FUV0136..... | 92.9 | B5 | 1615 | 225 |
| FUV0137..... | 473.0 | B5 | 1615 | 225 |
| FUV0138..... | 17.4 | B5 | 1615 | 225 |
| NUV0070..... | 112.0 | A2 | 1892 | 412 |
| NUV0072..... | 22.0 | A2 | 1892 | 412 |
| NUV0073..... | 112.0 | A4 | 2205 | 244 |
| NUV0127..... | 95.0 | A5 | 2558 | 456 |
| NUV0128..... | 472.0 | A5 | 2558 | 456 |
| NUV0129..... | 18.3 | A5 | 2558 | 456 |

using Space Telescope guide stars as astronomic standards (Lasker et al. 1990).

Figure 1*a* (Plate 25) shows the 9.7 × 9.7 section of UIT image NUV0128, the 472 s A5 (2558 Å) exposure, centered on R136 and resampled to a north-up, east-left orientation. The insert is from the 95.0 s A5 exposure NUV0127. Figure 1*b* (Plate 26) shows the same field extracted from the 473 s B5 exposure FUV0137, with a central insert from the 92.9 s exposure FUV0136. The FWHM of Gaussian fits to the core of the UIT PSF on these images is 2.″5–3.″0. Figure 2*a* (Plate 28) shows the corresponding field from our *R*-band image, which was obtained with a 2048 × 2048 CCD and resampled to the same orientation and scale as Figure 1. Nebular emission is present in both the UIT image and the ground-based image. The diffuse ultraviolet nebular emission arises almost entirely from dust-scattered stellar continuum, with a small contribution from two-photon recombination emission, while the *R*-band nebular emission is presumably mainly from Hα.

## 3. PHOTOMETRY

IDL implementations of DAOPHOT (Stetson 1987) algorithms are used to locate stars and perform aperture and PSF-fit photometry. Aperture photometry uses an aperature of radius 3.″4 (3 px). PSF-fit photometry uses a 3.″4 fitting radius, with a PSF determined for each image from 12 isolated stars of about the same aperture magnitude, near the midpoint of the magnitude range for the image. The *B* photometry uses aperture and fitting radii of 1.″6 (2 px). Zero points for the UV magnitudes are determined using *IUE* spectra, while the zero point of the *B*-magnitudes is determined from Parker's photometry (1992) of 21 bright 30 Dor stars.

Combined aperture and calibration correlations for the UIT magnitudes are determined by averaging *IUE* spectra of seven bright stars in the Sanduleak catalog (1969), over the UIT filter functions to compute expected magnitudes in the UIT bands. These *IUE* spectra were used by Fitzpatrick (1985) in his investigations of the 30 Dor extinction curve. The *IUE* spectra were reduced using the standard corrections for the sensitivity degradation of the cameras, although the Fanelli et al. spectral atlas used the newer Bohlin & Grillmair (1988) corrections for the sensitivity degradation of the LWR camera. This slight inconsistency in the treatment of the *IUE* spectra only affects the UIT magnitudes by a few 0.01 mag, and thus has little or no effect on the spectral type and reddening fits discussed later. The star names and the numbers of the *IUE* spectra are given in Table 2.

The additive constants necessary to adjust the UIT magnitudes to bring them into agreement with the *IUE* fluxes of the seven stars are computed for each image separately. The average adjustment is then applied to all magnitudes computed from that image. The standard deviation of the mean adjustment is about 0.05 mag for each of the four bands, for each of the images used in each band.

TABLE 2

STARS AND *IUE* SPECTRA USED IN DETERMINATION OF APERTURE CORRECTION

| Sanduleak | *IUE* Spectrum |
|---|---|
| 129-68..... | SWP 22483 |
| 129-68..... | LWR 17287 |
| 265-69..... | SWP 19560 |
| 265-69..... | LWR 15593 |
| 140-68..... | SWP 8896 |
| 140-68..... | LWR 7654 |
| 213-69..... | SWP 4913 |
| 213-69..... | LWR 4234 |
| 228-69..... | SWP 8927 |
| 228-69..... | LWR 7676 |
| 256-69..... | SWP 4968 |
| 256-69..... | LWR 4302 |
| 270-69..... | SWP 17184 |
| 270-69..... | LWR 13467 |

A final check on the UIT photometric accuracy is performed by comparing the corrected UIT magnitudes with magnitudes obtained from another independent set of *IUE* spectra for four 30 Dor stars in our field: R133, R135, R139, and R140. The mean difference obtained between the UIT B5 and A5 magnitudes and magnitudes computed by averaging the *IUE* spectra over the UIT filter curves is 0.033 mag, with standard deviation 0.103 mag. Therefore, 0.10 mag is our estimate for the uncertainty in the magnitudes relative to the *IUE* flux scale, as previously adopted for UIT photometry of stars in NGC 206 (Hill et al. 1992). Our estimate of the uncertainty in the *B*-magnitudes is 0.05–0.10 mag.

Because of the differing sensitivities of the bandpasses, varying numbers of stars are measured in the different bands: 314 are measured in the A5 band, 313 in B5, 165 in A2, and 75 in A4. *B*-magnitudes are obtained for 308 stars from a CCD image. Table 1 includes the central wavelengths and bandwidths of each of the UIT filters.

UIT magnitudes are defined by the relation $m_{\rm UIT} = -2.5 \times \log f_{\rm UIT} - 21.1$, where $f_{\rm UIT}$ is the average stellar flux over the band in units ergs (cm$^2$ Å s)$^{-1}$. B5 band magnitudes range from $m_{162} = 8.45$ to 15.87, while A5 band magnitudes range from $m_{256} = 9.58$ to 16.65. *B*-magnitudes range from 11.41 to 18.41. Histograms of the magnitudes measured in each band are plotted in Figure 3.

Equatorial coordinates of the stars are determined by locating them on the ground-based Strömgren *u* image, for which an astrometric solution is found using space telescope guide stars as standards. The estimated errors in the positions are less than 1″ relative to the guide star frame (Lasker et al. 1990). Table 3 gives the positions (R.A. and declination offsets in arcsec from R136, cols. [2] and [3]), and magnitudes $m_{162}$, $m_{189}$, $m_{221}$, $m_{256}$, and *B* in the UIT B5, A2, A4, A5, and optical B bands, respectively (cols. [4]–[8]). (Only a small portion of Table 3 is included here; the full table is distributed on CD-ROM). The equatorial coordinates (equinox J2000) for R136 are $\alpha_{2000} = 5^{\rm h}38^{\rm m}42^{\rm s}$ and $\delta_{2000} = -69°6'1''$. When a star is measured on more than one image in a given UIT band, the

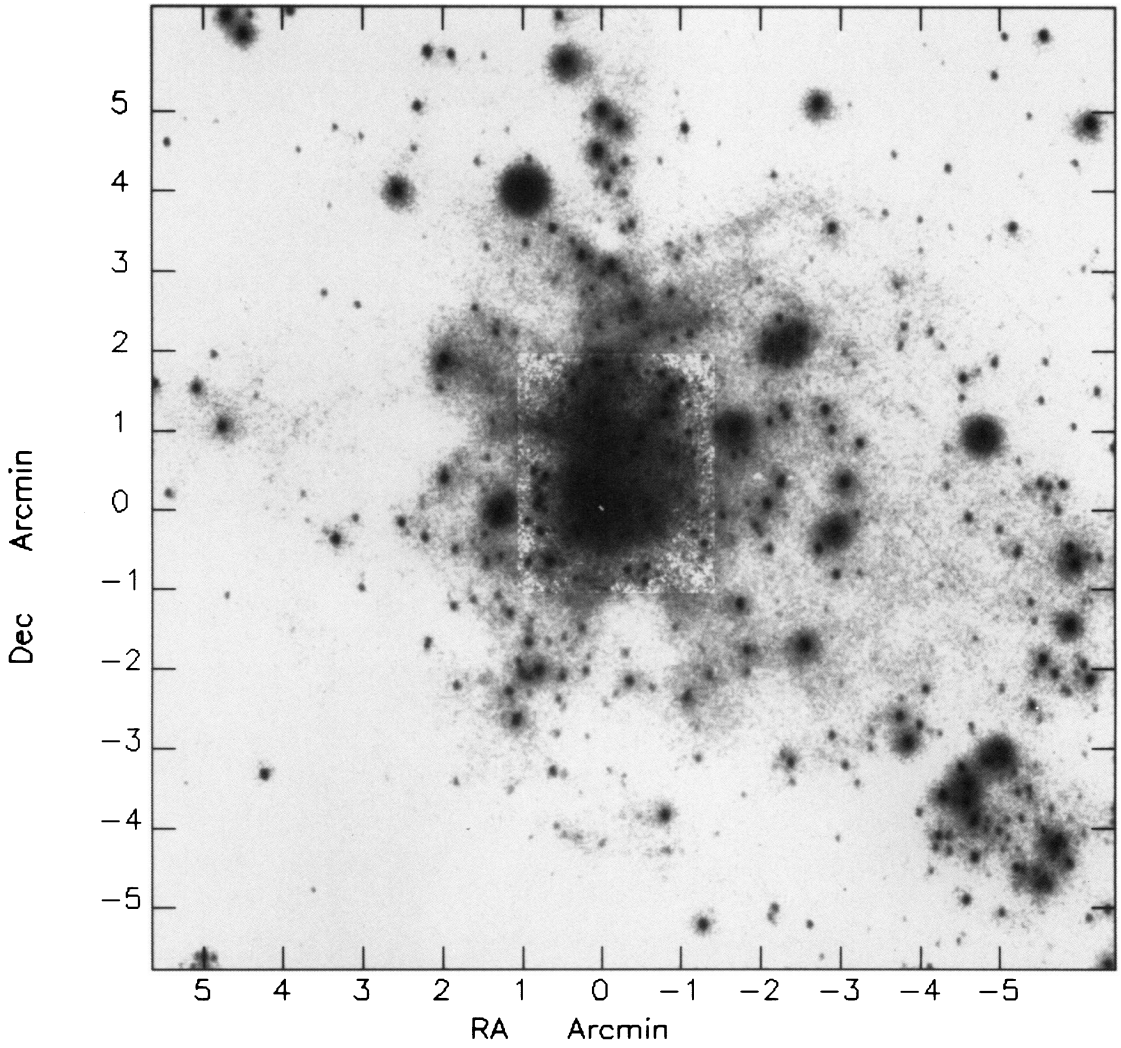


FIG. 1*a*

FIG. 1.—(*a*) 12′ × 12′ field centered on R136, extracted from 472 s A5 exposure NUV0128, with central region extracted from 92 s exposure NUV0127. (*b*) 12′ × 12′ field centered on R136 extracted from 473 s B5 exposure FUV0137, with central region extracted from 93 s exposure FUV0136. (*c*) Same as (*a*) with positions of measured stars indicated by circles.

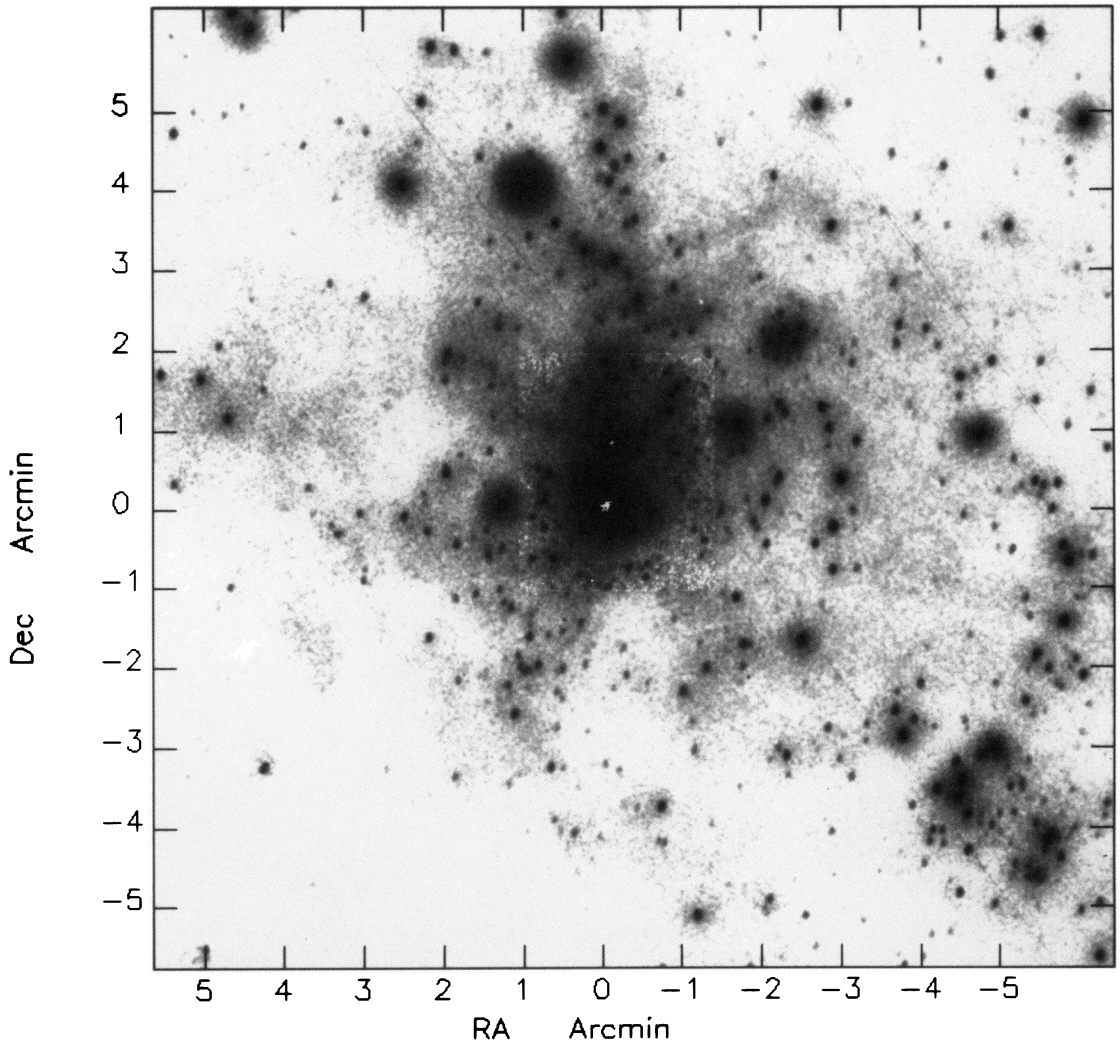


FIG. 1*b*

HILL et al. (see 413, 605)

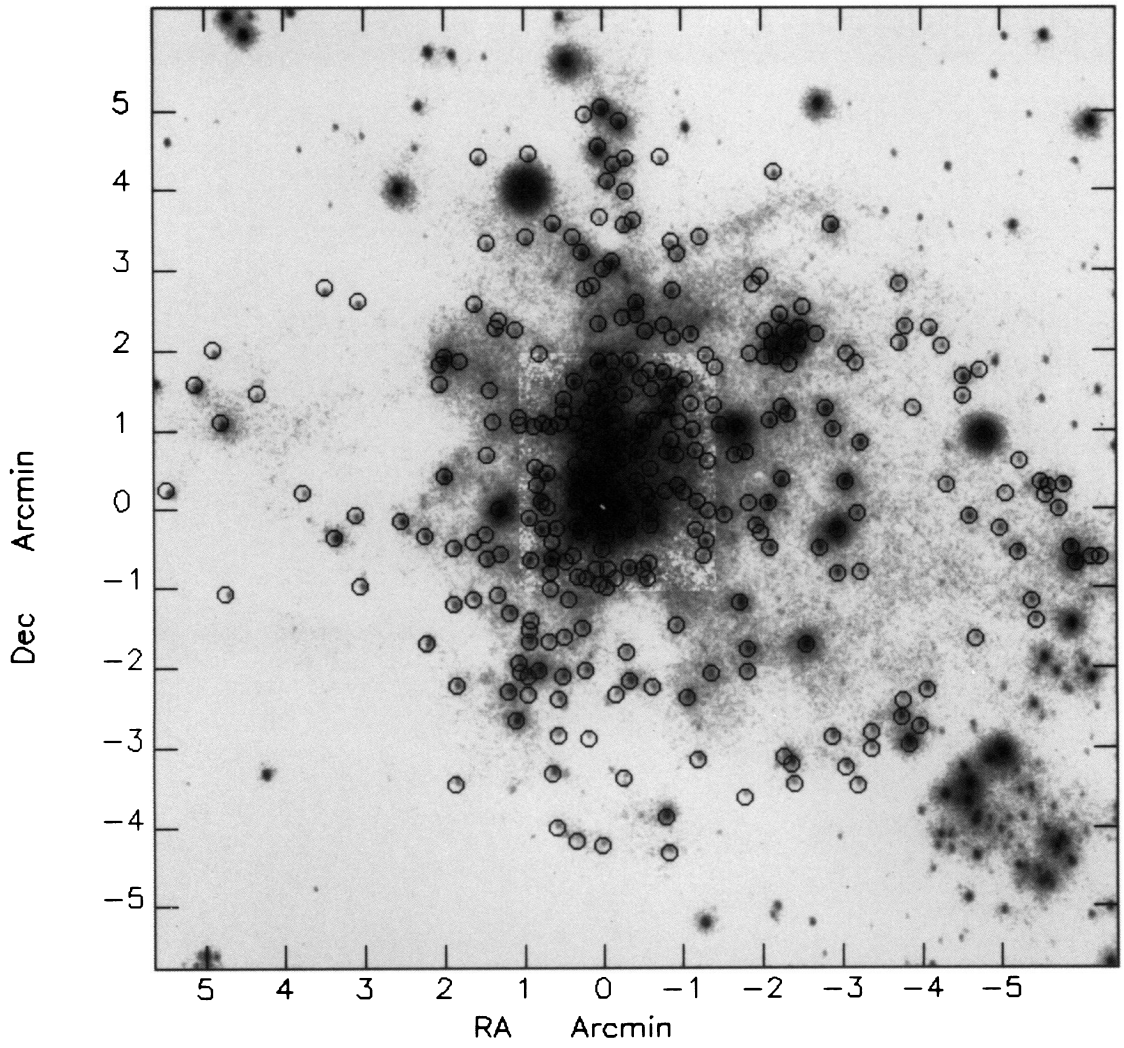


HILL et al. (see 413, 605)

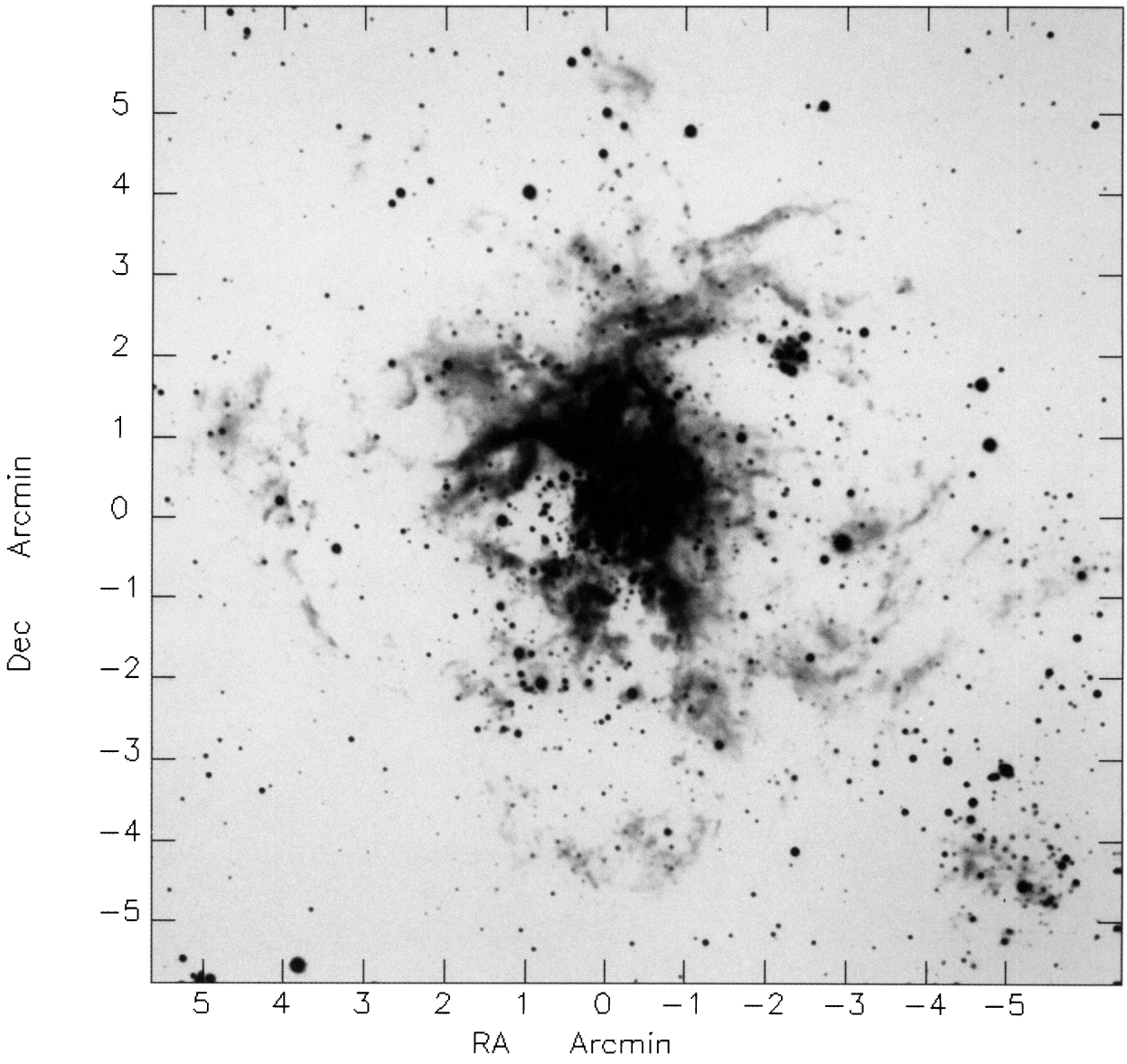


FIG. 2a

FIG. 2.—(*a*) 12′ × 12′ field registered with Fig. 1*a*–1*c*, extracted from *R*-band CCD image obtained at the Cerro Tololo Interamerican Observatory 0.9 m. Diffuse Hα emission is included in the band. (*b*) Same as (*a*), but stars having fit values of $E(B-V)_{FS}$ less than 0.03 marked with circles, and stars with fit values of $E(B-V)_{FS}$ greater than 0.30 marked with boxes.

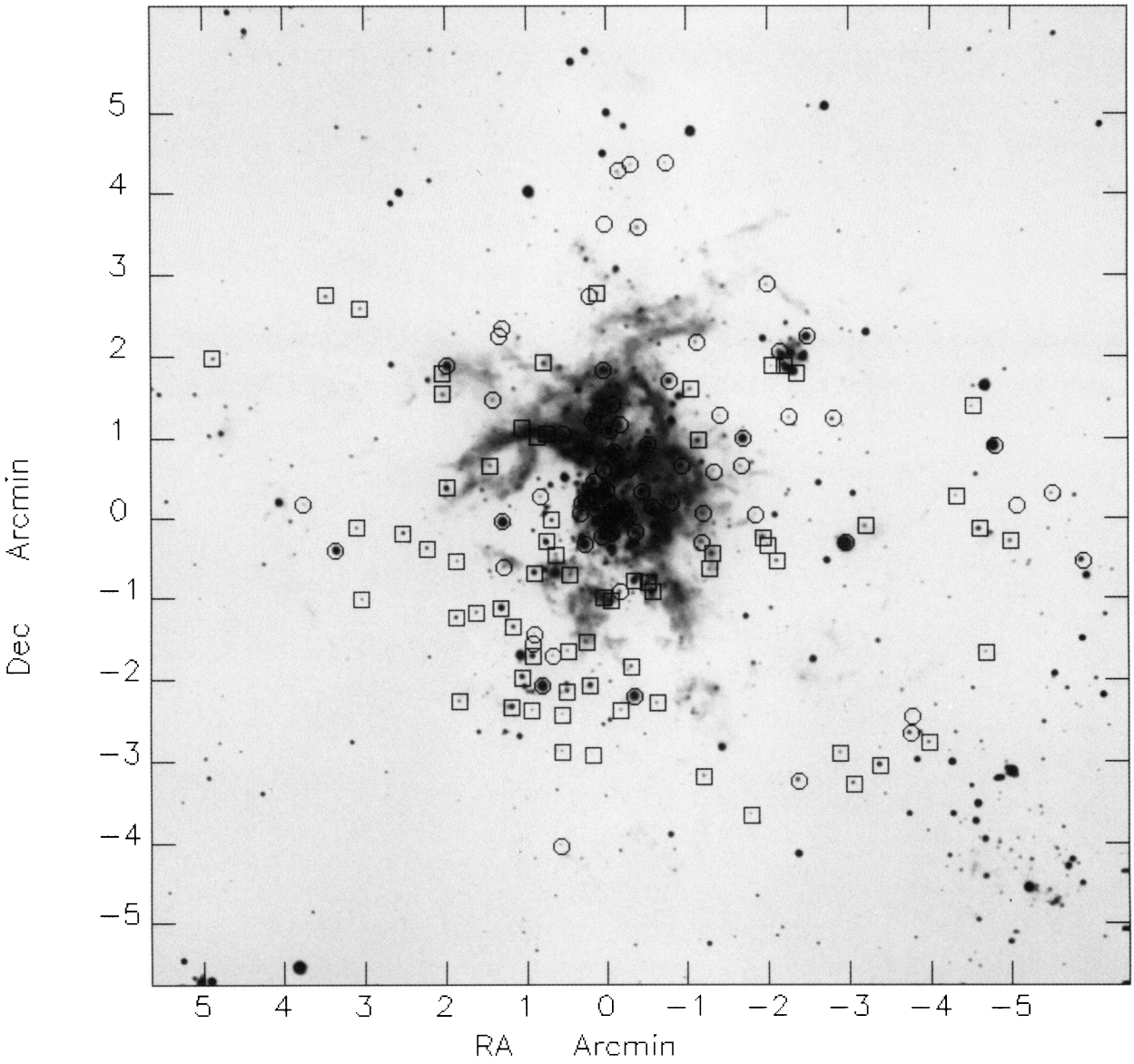


FIG. 2*b*

HILL et al. (see 413, 605)

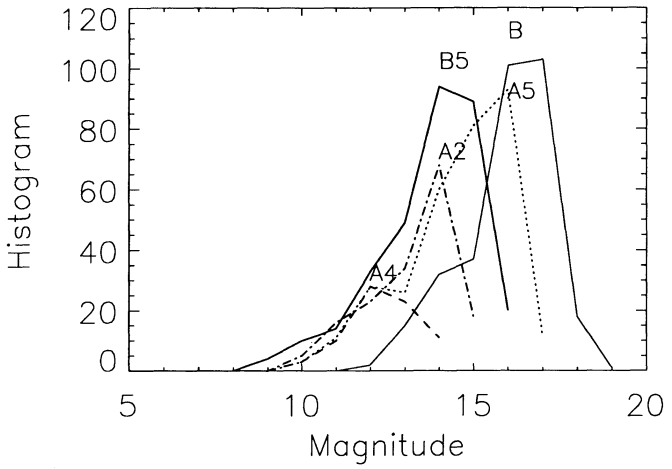


FIG. 3.—Histograms of magnitudes measured in the B5, A2, A4, A5, and B bands, in units of stars/mag.

measurement with largest estimated S/N is adopted. The magnitudes are not corrected for extinction. Table 3 does not contain an entry for R136, which is actually a cluster containing nearly 50 very early type stars, providing much of the ionizing radiation for the nebula (Campbell et al. 1992). R136 is unresolved in our images. The UIT fluxes for this object were previously discussed by Cheng et al. (1992). For cases in which no magnitude exists for a star in a given band, the magnitude is recorded as 99.00.

Before further analysis, the stellar magnitudes are corrected for foreground Galactic extinction [$E(B-V) = 0.06$] and LMC halo extinction [$E(B-V) = 0.04$] according to the reddening model for the region of Heap et al. (1991). These foreground extinction corrections are 0.82 mag in the B5 band, 0.82 mag in A2, 0.90 mag in A4, 0.73 mag in A5, and 0.41 mag in B. The corrections are determined by applying the Galactic extinction curve (Savage & Mathis 1979) and the general (i.e., non-30 Dor) LMC extinction curve (Fitzpatrick 1985) to a Kurucz (1992) model atmosphere with effective temperature 30,000 K and log surface gravity 4.0. (Because of the width of the UIT and *B*-filter curves, the corrections have a slight dependence on spectral type.) Further extinction is assumed to take place in 30 Dor, according to the 30 Dor reddening curve of Fitzpatrick (1985) (called the "F extinction curve" below), combined with the nebular extinction curve of Fitzpatrick & Savage (1984) (called the "FS extinction curve" below). The FS extinction curve differs from the F extinction curve primarily in the ratio of the far-UV extinction to the near-UV and optical extinction, with the ratio of B5 extinction to A5 extinction lower by 36% (cf. Fig. 4).

Spectral types and extinctions for individual stars are determined by comparison to a set of *IUE* standard spectra using a least-squares minimization technique. Fanelli et al. (1992) compiled a library of mean ultraviolet stellar energy distributions derived from *IUE* spectrophotometry of 218 Galactic stars, which are divided into 56 groups by spectral type and luminosity class. The spectral type groups important for our investigation are O3-6 V, O7-B0 V, B1-1.5 V, B2-4 V, O9-B0 IV, B2-5 IV O5-6 III, B0-2 III, B3-6 III, O4-9 I, B0-2 I, B3-5 I, B6-9 I, and A0-2 I. The spectra of these groups are averaged over the UIT bandpasses and the resulting $m_{\rm UIT} - V$ colors determined. Ultraviolet colors for the spectral library will be presented elsewhere (Fanelli et al. 1993, in preparation), along with a discussion of the overall morphology of the UV color-magnitude and color-color diagrams.

The $m_{\rm UIT} - V$ colors are combined with the absolute *V*-magnitudes, $B-V$ colors, and the distance modulus 18.57 to compute the predicted magnitudes in the UIT bands and the *B* band for unreddened stars in the Fanelli et al. spectral class bins. Panagia et al. (1991) determined a distance modulus to supernova 1987a of 18.55, and suggested that the 30 Dor stars have a slightly larger distance. Heap et al. (1991) used the distance modulus 18.57 in their investigation of Melnick 42.

We then use the F and FS reddening curves to determine magnitudes in all five bands for the 14 spectral type bins. We adopt F curve $E(B-V)$ values ranging from 0.09 and 0.16 mag, combined with FS curve $E(B-V)$ ranging from 0.00 to 0.60 mag. We therefore have a set of 14 × 480 reddened standard

TABLE 3

30 DOR STELLAR *UV* AND *B* PHOTOMETRY

| UIT (1) | *X* (2) | *Y* (3) | $m_{162}$ (4) | $m_{189}$ (5) | $m_{221}$ (6) | $m_{256}$ (7) | *B* (8) |
|---|---|---|---|---|---|---|---|
| 0.... | −49.1 | −261.0 | 14.58 | 99.00 | 99.00 | 15.58 | 16.43 |
| 1.... | 0.6 | −256.1 | 15.34 | 99.00 | 99.00 | 15.74 | 17.08 |
| 2.... | 20.2 | −251.9 | 14.08 | 99.00 | 99.00 | 15.17 | 16.39 |
| 3.... | 35.7 | −241.5 | 14.64 | 99.00 | 99.00 | 15.74 | 16.58 |
| 4.... | −46.3 | −234.1 | 12.52 | 12.83 | 13.06 | 13.06 | 14.21 |
| 5.... | −105.7 | −218.9 | 15.60 | 99.00 | 99.00 | 16.05 | 16.33 |
| 6.... | −191.3 | −210.6 | 14.28 | 14.59 | 99.00 | 15.60 | 16.51 |
| 7.... | −142.7 | −209.2 | 14.75 | 99.00 | 99.00 | 15.55 | 16.92 |
| 8.... | 111.1 | −209.2 | 14.47 | 99.00 | 99.00 | 15.53 | 16.38 |
| 9.... | −14.8 | −204.8 | 15.15 | 99.00 | 99.00 | 16.33 | 16.77 |
| 10.... | 38.1 | −201.2 | 13.20 | 13.75 | 99.00 | 14.38 | 15.43 |
| 11.... | −181.9 | −196.2 | 14.44 | 99.00 | 99.00 | 14.87 | 15.49 |
| 12.... | −140.9 | −193.9 | 12.89 | 13.18 | 13.14 | 13.50 | 15.10 |
| 13.... | −71.0 | −190.9 | 14.39 | 99.00 | 99.00 | 15.22 | 16.02 |
| 14.... | −134.8 | −188.5 | 14.31 | 99.00 | 99.00 | 15.53 | 16.70 |
| 15.... | −201.3 | −182.8 | 14.80 | 99.00 | 99.00 | 15.42 | 15.07 |
| 16.... | −229.4 | −179.1 | 10.97 | 11.55 | 11.67 | 11.85 | 13.76 |
| 17.... | 11.4 | −175.1 | 15.87 | 99.00 | 99.00 | 16.23 | 16.47 |
| 18.... | −172.2 | −173.7 | 13.87 | 13.92 | 99.00 | 14.71 | 15.82 |
| 19.... | 34.3 | −172.3 | 15.13 | 99.00 | 99.00 | 15.78 | 16.07 |
| 20.... | −201.7 | −170.3 | 14.43 | 99.00 | 99.00 | 15.38 | 16.36 |
| 21.... | −238.0 | −166.2 | 13.37 | 13.90 | 99.00 | 14.02 | 15.36 |
| 22.... | 65.7 | −161.5 | 12.85 | 12.89 | 12.88 | 13.22 | 14.11 |
| 23.... | −223.5 | −159.2 | 12.62 | 99.00 | 12.82 | 13.18 | 14.86 |
| 24.... | 34.0 | −145.2 | 14.66 | 99.00 | 99.00 | 15.25 | 16.12 |
| 25.... | −225.3 | −146.1 | 14.54 | 99.00 | 99.00 | 15.81 | 16.80 |
| 26.... | −62.9 | −144.2 | 12.99 | 13.53 | 99.00 | 14.26 | 15.71 |
| 27.... | −9.5 | −141.9 | 15.27 | 99.00 | 99.00 | 15.84 | 16.13 |
| 28.... | 56.4 | −142.1 | 15.22 | 99.00 | 99.00 | 15.91 | 16.15 |
| 29.... | 71.3 | −139.6 | 13.80 | 99.00 | 99.00 | 14.03 | 14.58 |
| 30.... | −243.0 | −138.7 | 13.45 | 13.80 | 99.00 | 13.96 | 15.72 |
| 31.... | −36.2 | −136.8 | 15.10 | 99.00 | 99.00 | 15.57 | 16.27 |
| 32.... | 110.8 | −135.5 | 14.50 | 99.00 | 99.00 | 14.91 | 15.91 |
| 33.... | −19.4 | −131.7 | 14.36 | 99.00 | 99.00 | 13.68 | 13.21 |
| 34.... | 56.4 | −128.9 | 13.60 | 13.71 | 99.00 | 14.41 | 15.17 |
| 35.... | 30.5 | −128.0 | 14.03 | 99.00 | 99.00 | 14.55 | 15.16 |
| 36.... | −80.4 | −126.5 | 13.30 | 13.41 | 99.00 | 14.82 | 15.49 |
| 37.... | 62.0 | −124.9 | 13.84 | 99.00 | 99.00 | 14.14 | 15.78 |
| 38.... | −107.9 | −125.1 | 14.12 | 99.00 | 99.00 | 15.22 | 16.51 |
| 39.... | 13.2 | −123.9 | 14.76 | 99.00 | 99.00 | 15.01 | 14.85 |
| 40.... | 48.7 | −124.4 | 13.35 | 13.45 | 99.00 | 12.84 | 12.37 |
| 41.... | 63.8 | −117.7 | 14.34 | 99.00 | 99.00 | 14.70 | 14.77 |
| 42.... | −17.1 | −110.1 | 14.91 | 99.00 | 99.00 | 15.60 | 15.90 |
| 43.... | −108.1 | −108.0 | 13.07 | 13.39 | 99.00 | 13.74 | 15.36 |
| 44.... | −152.4 | −104.9 | 11.07 | 11.59 | 11.77 | 11.93 | 13.53 |
| 45.... | 132.8 | −103.3 | 13.58 | 14.00 | 99.00 | 14.12 | 15.51 |
| 46.... | 41.3 | −102.4 | 14.76 | 99.00 | 99.00 | 15.98 | 16.54 |
| 47.... | 56.0 | −102.5 | 13.54 | 13.75 | 99.00 | 13.66 | 14.51 |
| 48.... | −280.1 | −99.9 | 15.10 | 99.00 | 99.00 | 15.75 | 16.36 |
| 49.... | 30.1 | −98.7 | 14.55 | 99.00 | 99.00 | 15.63 | 16.23 |

TABLE 4

$A_{UIT}/E(B-V)$ FOR THE EXTINCTION CURVES USED

| Curve | $A_{162}/E(B-V)$ | $A_{189}/E(B-V)$ | $A_{221}/E(B-V)$ | $A_{256}/E(B-V)$ |
|---|---|---|---|---|
| Galactic | 8.06 | 8.11 | 9.13 | 7.34 |
| LMC | 8.49 | 8.36 | 8.74 | 7.17 |
| 30 Dor (F) | 9.93 | 9.18 | 8.79 | 7.26 |
| 30 Dor Neb. (FS) | 7.51 | 7.54 | 8.02 | 6.42 |

energy distributions against which to compare the energy distribution of each individual star. The factors $A_{UIT}/E(B-V)$ relating $E(B-V)$ to the extinctions in the B5, A2, A4, and A5 bands are given in Table 4, for each of the extinction curves used in this investigation.

For each of the 314 stars, we estimate the F curve extinction, the FS curve extinction, and spectral type as that combination which minimizes the rms magnitude difference between the model and the observations. Figure 4 plots $A_{UIT}/E(B-V)$ versus wavelength for the F, FS, and Galactic extinction curves. The F and FS curves are sufficiently different that the effects of extinction following each curve can be distinguished.

The UIT star number, estimated spectral type, estimated F curve $E(B-V)$, estimated FS curve $E(B-V)$, and the rms magnitude differences between the best-fit model and the observations are given in columns (1)–(5) of Table 5. (Only a small portion of Table 5 is included here; the full table is distributed on CD-ROM.) The average of the estimated values of the F curve $E(B-V)$ is 0.11, and the average of the estimated values of the FS curve $E(B-V)$ is 0.17. The rms variations in the extinction are 0.02 for $E(B-V)_F$ and 0.17 for $E(B-V)_{FS}$. These averages agree well with the two-component extinction model for 30 Dor of Fitzpatrick & Savage (1984). The fit values of the total A5 band extinction range from 0.65 to 5.01 mag.

Figure 5*a* is the observed color-magnitude diagram (CMD) constructed from the $m_{162} - B$ colors and $m_{162}$ magnitudes for 308. No extinction has been removed. Positions of the library spectral standards are also given in Figures 5*a* and 5*b*, both for the cases of foreground extinction only, and for the mean internal 30 Dor extinction values of $E(B-V)_F = 0.11$ and $E(B-V)_{FS} = 0.17$, in addition to the foreground extinction. Figure 5*b* shows the unreddened (in 30 Dor) dwarfs as circles, connected by dashed lines, while unreddened supergiants are plotted as circles, connected by dotted lines. Reddened dwarfs are shown as squares, connected by dashed lines, while reddened supergiants are plotted as squares connected by dotted lines. The separation between the dot-dash reddening line connecting unreddened O3-6 V stars with reddened stars

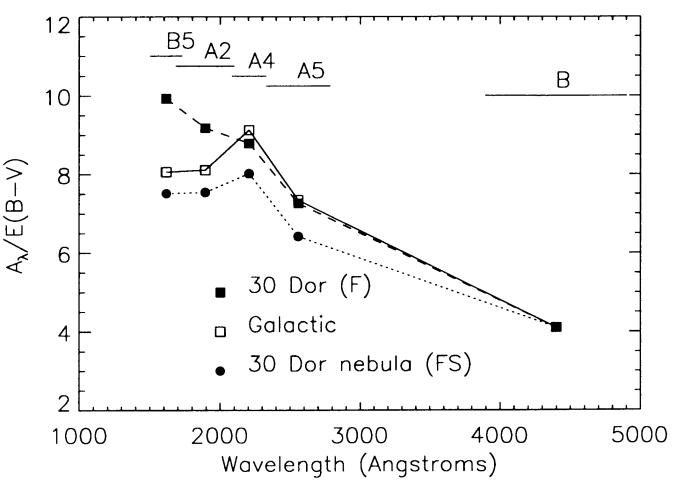


FIG. 4.—$A_{UIT}/E(B-V)$ vs. wavelength for the F, FS, and Galactic extinction curves. Approximate wavelength ranges of the filters are shown by the horizontal lines.

TABLE 5

FIT SPECTRAL TYPES AND EXTINCTIONS

| UIT (1) | Spectral Type (2) | $E(B-V)_F$ (3) | $E(B-V)_{FS}$ (4) | RMS (5) |
|---|---|---|---|---|
| 0..... | B1-1.5 V | 0.13 | 0.11 | 0.28 |
| 1..... | B1-1.5 V | 0.15 | 0.17 | 0.08 |
| 2..... | B1-1.5 V | 0.09 | 0.10 | 0.19 |
| 3..... | B2-5 IV | 0.09 | 0.00 | 0.24 |
| 4..... | O5-6 III | 0.16 | 0.26 | 0.16 |
| 5..... | O9-B0 IV | 0.10 | 0.58 | 0.14 |
| 6..... | B1-1.5 V | 0.09 | 0.13 | 0.30 |
| 7..... | B1-1.5 V | 0.09 | 0.18 | 0.09 |
| 8..... | B1-1.5 V | 0.12 | 0.11 | 0.30 |
| 9..... | B2-5 IV | 0.09 | 0.06 | 0.32 |
| 10..... | O7-B0 V | 0.09 | 0.25 | 0.23 |
| 11..... | O5-6 III | 0.13 | 0.58 | 0.08 |
| 12..... | B0-2 III | 0.15 | 0.01 | 0.14 |
| 13..... | O7-B0 V | 0.09 | 0.39 | 0.20 |
| 14..... | B1-1.5 V | 0.09 | 0.15 | 0.26 |
| 15..... | B0-2 I | 0.11 | 0.60 | 0.44 |
| 16..... | O5-6 III | 0.14 | 0.11 | 0.14 |
| 17..... | O9-B0 IV | 0.11 | 0.60 | 0.12 |
| 18..... | O7-B0 V | 0.09 | 0.31 | 0.20 |
| 19..... | O9-B0 IV | 0.09 | 0.54 | 0.21 |
| 20..... | B1-1.5 V | 0.16 | 0.05 | 0.24 |
| 21..... | O3-6 V | 0.09 | 0.43 | 0.08 |
| 22..... | B0-2 I | 0.15 | 0.23 | 0.31 |
| 23..... | B0-2 III | 0.12 | 0.01 | 0.01 |
| 24..... | O7-B0 V | 0.12 | 0.38 | 0.11 |
| 25..... | B2-4 V | 0.09 | 0.00 | 0.29 |
| 26..... | O7-B0 V | 0.09 | 0.23 | 0.28 |
| 27..... | O9-B0 IV | 0.09 | 0.55 | 0.18 |
| 28..... | O9-B0 IV | 0.09 | 0.55 | 0.22 |
| 29..... | O4-9 I | 0.16 | 0.53 | 0.10 |
| 30..... | O7-B0 V | 0.10 | 0.24 | 0.12 |
| 31..... | O9-B0 IV | 0.09 | 0.53 | 0.07 |
| 32..... | O9-B0 IV | 0.09 | 0.47 | 0.05 |
| 33..... | A0-2 I | 0.13 | 0.00 | 0.16 |
| 34..... | O9-B0 IV | 0.11 | 0.29 | 0.21 |
| 35..... | O5-6 III | 0.15 | 0.50 | 0.15 |
| 36..... | O7-B0 V | 0.09 | 0.26 | 0.47 |
| 37..... | O7-B0 V | 0.15 | 0.22 | 0.15 |
| 38..... | B1-1.5 V | 0.09 | 0.11 | 0.18 |
| 39..... | B0-2 I | 0.09 | 0.59 | 0.26 |
| 40..... | B6-9 I | 0.16 | 0.01 | 0.53 |
| 41..... | O4-9 I | 0.16 | 0.60 | 0.24 |
| 42..... | O3-6 V | 0.12 | 0.60 | 0.23 |
| 43..... | O7-B0 V | 0.11 | 0.18 | 0.02 |
| 44..... | O5-6 III | 0.16 | 0.09 | 0.14 |
| 45..... | B0-2 III | 0.09 | 0.19 | 0.07 |
| 46..... | B2-5 IV | 0.09 | 0.01 | 0.32 |
| 47..... | O4-9 I | 0.16 | 0.49 | 0.08 |
| 48..... | O9-B0 IV | 0.09 | 0.54 | 0.17 |
| 49..... | O7-B0 V | 0.09 | 0.44 | 0.32 |

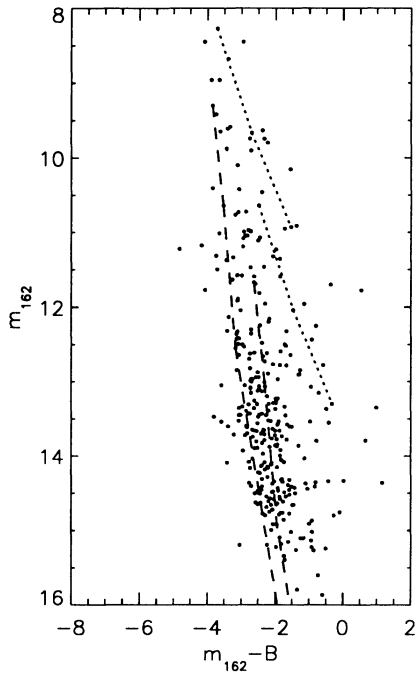


FIG. 5a

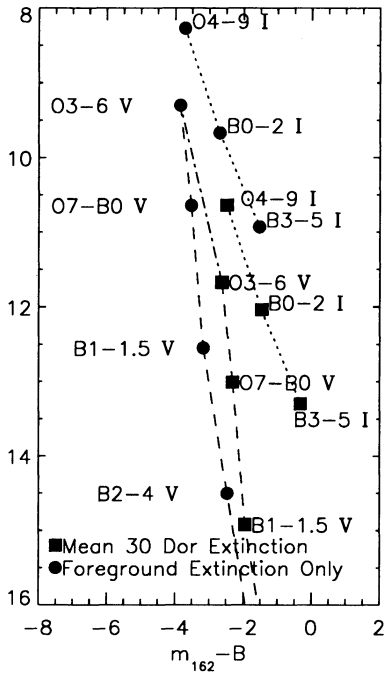


FIG. 5b

FIG. 5.—(*a*) Observed $m_{162} - B$ vs. $B$ CMD for 308 stars. No extinction has been removed. Dotted and dashed lines marking the positions of spectral standards are as in *b*. (*b*) Expected positions in the $m_{162} - B$ vs. $B$ plane of Fanelli et al (1992) spectral library spectral types, plotted as circles for the case of foreground extinction only, and as boxes in the case of average 30 Dor extinction. Dwarfs are connected by dashes, while supergiants are connected by dots. The slope of a reddening line is indicated by the dot-dash line connecting the position and unreddened (except for foreground reddening) O3-6 V star with the position of the O3-6 V star with average reddening.

of the same type, and the line of increasing spectral type enables the simultaneous determination of spectral type and extinction. Figure 5*a* shows only the positions of the observed stars and the lines from Figure 5*b* to allow the reader to judge the level of agreement.

It is perhaps surprising that the variance of the estimated values of $E(B-V)_{FS}$ is so high, since Fitzpatrick & Savage (1984) model the nebular extinction component as a uniform layer with $E(B-V) = 0.18$. However, their model is based on *IUE* spectra of very few stars, In the two-component extinction model of Fitzpatrick & Savage (1984), the nebular curve is supposed to apply to the material in the core of the nebula, which is behind the material whose extinction follows the F curve. We find that the amount of nebular extinction varies systematically over the field, as illustrated in Figure 2*b*. Large values of $E(B-V)_{FS}$ (greater than 0.3) occur predominantly outside a region of low extinction in the high surface brightness core of the 30 Dor nebula. The smallest values of $E(B-V)_{FS}$ (less than 0.03) are mostly along a north-south line extending from about 1′ south of R136 to about 4′ north, in a band about 2′ wide. This finding is in agreement with Fitzpatrick & Savage's (1984) determination that the stars R133, R139, and R140 have low nebular reddening. The UIT numbers for these stars are 192, 204, and 180. The corresponding $E(B-V)_{FS}$ values are 0.0 for all three stars.

Figure 2*b* marks stars with values of $E(B-V)_{FS}$ less than 0.03 with a circle, while stars with fit values greater than 0.30 are marked with a square. The systematic dependence of the degree of nebular extinction on location in the nebula is evident. The low nebular reddening in the high surface brightness part of the nebula may be a result of dust grains having been expelled by stellar winds. Alternatively, stars in the outer parts of the nebula may lie behind or within dust clouds. The morphology of the nebular features in Figure 2, the *R*-band image, suggests that this may be the case.

Table 6 gives the number of stars fit to each of the spectral type bins in the library of Fanelli et al. (1992). Approximately 35% of the stars are fitted to main-sequence spectral types earlier than B1. Melnick (1985) has tabulated spectral types for 44 stars in common with stars from Tables 3 and 5. For these stars, plus seven others, Table 7 compares our photometric spectral type estimates with those from slit spectroscopy. Estimated spectral types are determined for 39 non-WR stars from slit spectra. For 34 of these stars the difference between the fit spectral type and the slit spectral type is at most one Fanelli et al. (1992) spectral class bin and two luminosity classes. For 13

TABLE 6

SPECTRAL TYPES AND THE NUMBER OF STARS FIT

| Spectral Type Bin | Number Fit |
|---|---|
| O3-6 V | 35 |
| O7-B0 V | 75 |
| B1-1.5 V | 89 |
| B2-4 V | 3 |
| O9-B0 IV | 14 |
| B2-5 IV | 15 |
| O5-6 III | 28 |
| B0-2 III | 12 |
| B3-6 III | 2 |
| O4-O9 I | 17 |
| B0-2 I | 13 |
| B3-5 I | 7 |
| B6-9 I | 2 |
| A0-2 I | 2 |

TABLE 7

MELNICK STARS: SPECTRAL TYPES AND FIT SPECTRAL TYPES

| Star | UIT | Melnick Spectral Type | Fit Spectral Type |
|---|---|---|---|
| B | 33 | A0 Ia | A0-2 I |
| R143 | 40 | F7 Ia | B6-9 I |
| Mk 70 | 57 | O8.5 V[a] | B0-2 I |
| Mk 53 | 68 | WN 8 | B0-2 I |
| Mk 51 | 77 | O4 If | O4-9 I |
| Mk 52 | 78 | B1 Ia | B3-5 I |
| Mk 11 | 82 | B0.5 Ia | B0-2 I |
| Mk 4 | 83 | O3 V(f) | O5-6 III |
| Mk 38 | 100 | O9 I | O3-6 V |
| Mk 12 | 103 | B0.5 Ia | B0-2 I |
| Mk 49 | 107 | WN 7 | O5-6 III |
| Mk 5 | 108 | O9.5 I | O4-9 I |
| Mk 35s | 113 | O5 V | O5-6 III |
| Mk 37, 37w | 114 | O4 If, WN 7 | O5-6 III |
| Mk 54 | 120 | B0.5 Ia | B0-2 I |
| R145 | 124 | WN 6 | O4-9 I |
| Mk 34 | 126 | WN 4.5 | O5.6 III |
| Mk 36 | 128 | O4 V | O3-6 V |
| Mk 80 | 131 | O9.5 I | O5-6 III |
| Mk 6 | 133 | O(7) V | O3-6 V |
| R138 | 136 | A0 Ia | B3-5 I |
| Mk 39 | 137 | O4 If | O4-9 I |
| R134 | 137 | WN 7 | ... |
| Mk 42 | 142 | O3 If | O4-9 I |
| Mk 15, 15s | 146 | O7 V, O4 V | O3-6 V |
| R141 | 149 | B0.5 I[b] | O4-9 I |
| Mk 32 | 151 | O8 II[b] | O5-6 III |
| R142 | 157 | B0 Ia | O4-9 I |
| Mk 24 | 160 | O7 V | O3-6 V |
| Mk 8 | 161 | O(?) V | O3-6 V |
| Mk 26 | 162 | O4 Vf | O3-6 V |
| Mk 27 | 165 | B0 I[b] | O5-6 III |
| Mk 47 | 175 | O5 If | O5-6 III |
| Mk 25 | 179 | O3 V | O5-6 III |
| R140N, S | 180 | WC5, WN4 | O4-9 I |
| R137 | 186 | B1 Ia | B0-2 I |
| Mk 60 | 188 | B0 I | O5-6 III |
| R133 | 192 | O7 pec | O4-9 I |
| Mk 57 | 201 | ... | O7-B0 V |
| R139 | 204 | O6Iaf | O4-9 I |
| Mk 23 | 210 | O(?) V | O3-6 V |
| R135 | 211 | WN6 | O4-9 I |
| Mk 29 | 220 | ... | O7-B0 V |
| Mk 59 | 223 | O(?) V | O3-6 V |
| Mk 58 | 227 | O8 V | O5-6 III |
| Mk 10 | 230 | O4 V | O5-6 III |
| Mk 21 | 232 | O7 V | O3-6 V |
| Mk 55 | 235 | O5 (f) | B0-2 III |
| Mk 22, 22W | 244 | O? + Of | O3-6 V |
| Mk 1 | 246 | B1 Ia | B3-5 I |
| B2 | 256 | A Ib | B3-5 I |
| R132 | 269 | B0.5 Ia | B3-5 I |

[a] Parker 1992.
[b] Walborn 1986.

stars our spectral type is equivalent to the spectral type determined spectroscopically. Melnick (1985) notes that many of the stellar spectra are contaminated by nebular emission, rendering classification difficult.

The mean of the rms magnitude residuals of the least-squares fits in Table 5 is 0.25 mag. Residuals of the size can not be accounted for by photometric error alone (estimated at 0.10 mag) or uncertainty in the spectral library magnitudes (also estimated at 0.10 mag). The largest remaining known sources of error are the uncertainty in the F and FS extinction curves, which Fitzpatrick (1985) estimates at $\sim 0.25$ in $(E_{\rm IUE} - V)/E(B-V)$, and the granularity in the Fanelli et al. (1992) spectral type bins, which can be estimated from Figures 5 and 6. Figure 6 plots magnitudes for the earliest library spectral types, for the case $E(B-V)_{\rm F} = 0.11$ and $E(B-V)_{\rm FS} = 0.17$. We believe that the rms residuals can be adequately accounted for by these extinction and sampling effects. It is unlikely that the somewhat lower metal abundance of the 30 Dor stars compared to the Galactic stars making up the spectral library of Fanelli et al. affects the spectral type and reddening fits. The $m_{\rm UIT} - V$ colors of model atmospheres with LMC metallicity are only a few 0.01 mag bluer than model atmospheres with solar metallicity for effective temperatures 20,000–30,000 K (Kurucz 1992).

As a test of the superiority of the F and FS extinction curves over the Galactic extinction curve for fitting the 30 Dor stars, spectral types and $E(B-V)$ are also estimated using the Galactic extinction curve for the 72 stars with magnitudes measured in all bands. The values of $E(B-V)$ are greater than 0.1 mag for 39 of the 72 stars. The rms magnitude residuals are greater for 85% of these stars, and the overall mean rms residual is 50% larger than in the case where the F and FS extinction curves are used.

## 4. INDIVIDUAL STARS

R143 is assigned type F7 Ia by Melnick and by Feast, Thackeray, & Wesselink (1960). The UIT magnitudes are fitted best to the B6-9 I spectral type bin. Parker et al. (1992) suggest that R143 is in fact a luminous blue variable (LBV), noting that its spectral type has apparently changed in the past 40 yr from a late F supergiant to an early B supergiant, then to a late B supergiant. The UIT B5 magnitude (from data obtained in 1990 December) is fainter than that derived from the *IUE* spectrum obtained in 1992 June by Parker et al. by $\sim 0.3$ mag. The UV color $m_{162} - m_{258}$ computed from magnitudes in the B5 and A5 bands is redder by $\sim 0.5$ mag than that obtained using the *IUE* spectrum, suggesting that the spectral type may have changed slightly since the time of the *Astro 1* mission.

The two very recently formed massive stars pointed out by Walborn & Blades (1987) correspond with UIT sources numbered 185 and 217, respectively. The least-squares fitting pro-

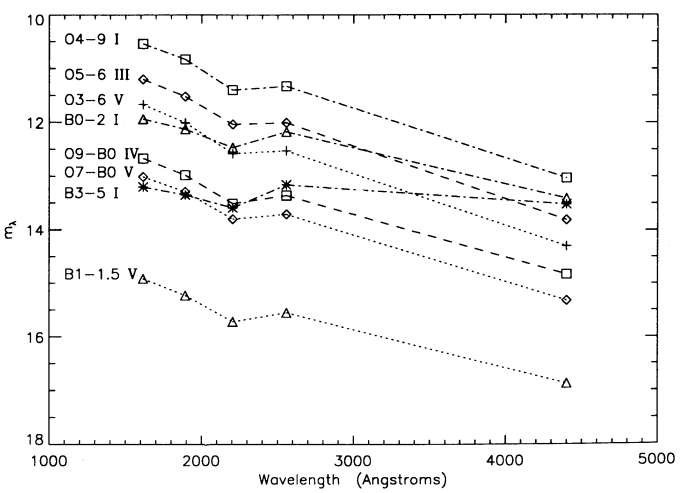


FIG. 6.—Magnitudes $m_{162}$, $m_{189}$, $m_{221}$, $m_{256}$, and $B$, for the earliest spectral types in the Fanelli et al. library, for distance modulus 18.57, $E(B-V)_{\rm F} = 0.11$ and $E(B-V)_{\rm FS} = 0.17$, in addition to the foreground Galactic and LMC halo extinction.

cedure gives estimated spectral types O3-6 V and O7-B0 V, with F curve $E(B-V) = 0.16$ and 0.09, and the FS curve $E(B-V) = 0.08$ and 0.20, respectively.

## 5. IMPLICATIONS FOR THE EVOLUTION OF THE UV EXTINCTION CURVE

We have confirmed that the wavelength dependence of the UV extinction for many stars in the 30 Dor region of the LMC is quantitatively different from that of the Galaxy. Instead, the local 30 Dor extinction follows a combination of the curves of Fitzpatrick (1985) and Fitzpatrick & Savage (1984). The Fitzpatrick (1985) extinction curve differs from the Galactic curve (Savage & Mathis 1979) in that the local maximum at 2200 Å, which was first found by one of us (Stecher 1965), is greatly suppressed. It also has higher extinction at the shorter UV wavelengths. The local maximum at 2200 Å was attributed to graphite by Stecher & Donn (1965) and to graphite and other kinds of carbonaceous material by many others.

The general assumption has been that the grains form in the atmospheres of evolved cool stars. The production of carbon grains in cool stellar atmospheres requires [C/O] > 1, to avoid having all the carbon tied up in CO, which probably does not happen until the "third dredge-up" brings carbon into the envelopes of evolved low-mass stars. Not until this happens will there be a sufficient number of carbonaceous grains in the interstellar medium to produce a strong 2200 Å peak.

The Galaxy is an evolutionarily older system than the 30 Dor region of the LMC; when stellar evolution and nucleosynthesis have progressed sufficiently, 30 Dor should also have a strong 2200 Å peak in its extinction curve. Interstellar shocks may also play a role in locally modifying grain structure and the extinction curve. Since heavy element abundance ratios are expected to depend on the star formation history (e.g., Gilmore & Wyse 1991), we would also expect the interstellar extinction curve to be affected. A detailed discussion of the chemical evolution of stellar systems with respect to their grain forming processes is beyond the scope of this paper, but should be carried out soon, since it now seems subject to observational test.

## 6. SUMMARY

UIT ultraviolet magnitudes in four bands, together with optical *B*-magnitudes, are presented for up to 314 early-type stars located in a 9.'7 × 9.'7 field centered on R136. The magnitudes have an rms uncertainty estimated at 0.10 mag from a comparison between the UIT magnitudes and *IUE* spectra. Spectral types and $E(B-V)$ color excesses are estimated using the *IUE* spectral library of Fanelli et al. (1992) and the 30 Dor extinction curves of Fitzpatrick (1985) and Fitzpatrick & Savage (1984). Most fit spectral types agree within one Fanelli et al. (1992) spectral type bin and two luminosity classes with the types determined by Melnick (1985) from optical slit spectra.

The mean color excesses following the two extinction curves agree well with the predictions of the two-component extinction model of Fitzpatrick & Savage (1984). However, the degree of nebular extinction is found to vary systematically by large amounts over the 30 Dor field. The minimum of nebular extinction in the central parts of the nebula suggests that dust has been expelled from this region by stellar winds. We also suggest that the form of the UV extinction curve can be understood as a consequence of the evolutionary state of the stellar population responsible for making the dust grains.

We gratefully acknowledge the innumerable contributions made by the many people involved in the *Astro 1* mission, including the many officials at NASA Headquarters whose support brought it through a long and difficult gestation period.

Funding for the UIT project has been through the Spacelab Office at NASA Headquarters under Project number 440-51. R. W. O. acknowledges NASA support of portions of this research through grants NAG5-700 and NAGW-2596 to the University of Virginia.

We thank Joel Offenberg for assisting with the pictures and Michael Greason for help with the tables. We also thank Joel Parker, the referee, for a very helpful report.

## REFERENCES

Bohlin, R. C., & Grillmair, C. J. 1988, 68, 487
Campbell, B., et al. 1992, AJ, 104, 1721
Cheng, K.-P., et al. 1992, ApJ, 395, L29
Fanelli, M. N., O'Connell, R. W., Burstein, D., & Wu, C.-C. 1992, ApJS, 82, 197
Fanelli, M. N., O'Connell, R. W., Hill, J. K., & Stecher, T. P. 1993, in preparation
Feast, M. W., Thackeray, A. D., & Wesselink, A. J. 1960, MNRAS, 121, 25
Fitzpatrick, E. L. 1985, ApJ, 299, 219
Fitzpatrick, E. L., & Savage, B. D. 1984, ApJ, 279, 578
Gilmore, G., & Wyse, R. F. G. 1991, ApJ, 367, L55
Heap, S. R., et al. 1991, ApJ, 377, L29
Hill, J. K., et al. 1992, ApJ, 395, L33
Kurucz, R. L. 1992, in The Stellar Populations of Galaxies, ed. B. Barbuy & A. Renzini (Dordrecht: Kluwer), 225
Lasker, B. M., Sturch, C. R., McLean, B. J., Russell, J. L., Jenker, H., & Shara, M. M. 1990, AJ, 99, 2019
Melnick, J. 1985, A&A, 153, 235
Panagia, N., Gilmozzi, R., Macchetto, F., Adorf, H.-M., & Kirshner, R. P. 1991, ApJ, 380, L23
Parker, J. W. 1992, Ph.D. thesis, Univ. Colorado
Parker, J. W., Clayton, G. C., Winge, C., & Conti, P. S. 1993, ApJ, , 409, 770
Sanduleak, N. 1969, Cerro Tololo Inter-American Obs. Contrib. No. 89
Savage, B. D., & Mathis, J. S. 1979, ARA&A, 17, 73
Stecher, T. P. 1965, ApJ, 142, 1683
Stecher, T. P., & Donn, B. 1965, ApJ, 142, 1681
Stecher, T. P., et al. 1992, ApJ, 395, L1
Stetson, P. B. 1987, PASP, 99, 101
Walborn, N. R. 1986, IAU Symp. 116, Luminous Stars and Associations in Galaxies, ed. C. W. H. de Loore, A. J. Willis, & P. Laskarides (Dordrecht: Reidel), 185
Walborn, N. R., & Blades, J. C. 1987, ApJ, 323, L65